

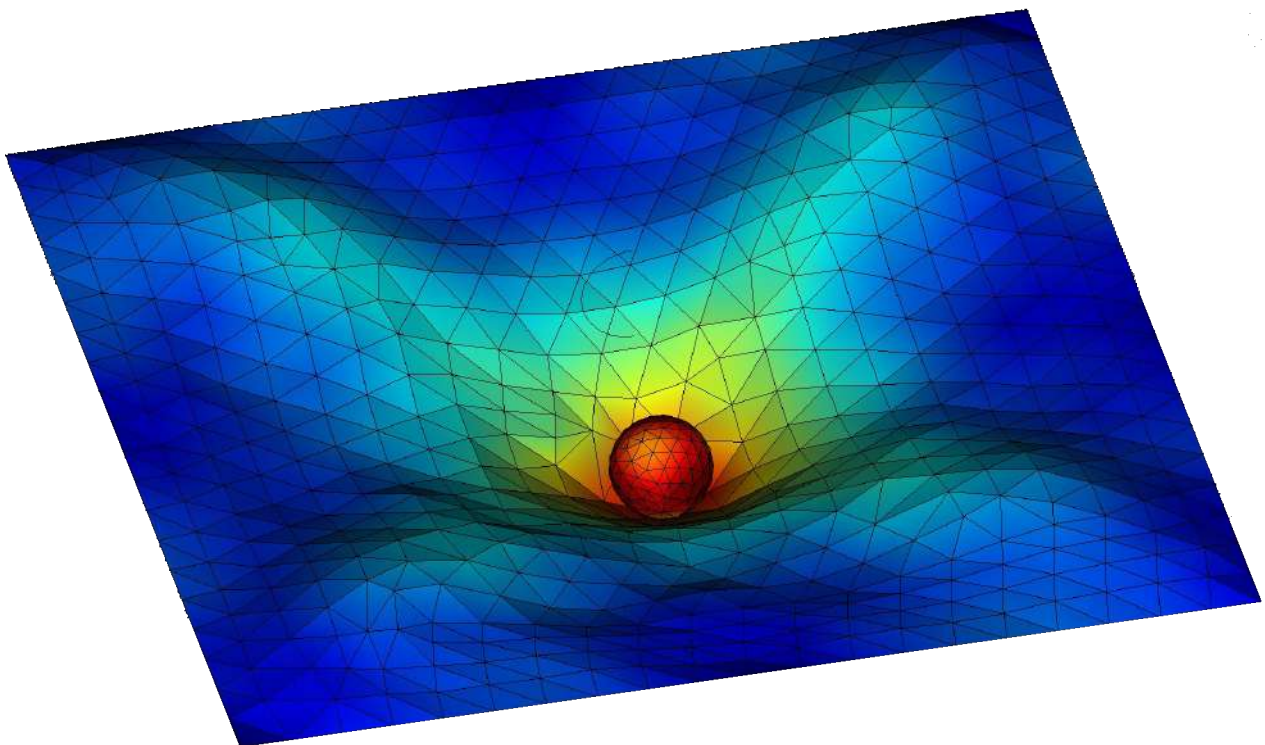
COMPDYN 2025

*10th International Conference
on Computational Methods in Structural Dynamics
and Earthquake Engineering*

PROCEEDINGS

Volume II

M. Papadrakakis, M. Fragiadakis (Eds.)



COMPADYN 2025

Computational Methods in Structural Dynamics and Earthquake Engineering

Proceedings of the 10th International Conference on Computational
Methods in Structural Dynamics and Earthquake Engineering
Held in Rhodes Island, Greece
15-18 June 2025

Edited by:

M. Papadrakakis

National Technical University of Athens, Greece

M. Fragiadakis

National Technical University of Athens, Greece

A publication of:

Institute of Structural Analysis and Antiseismic Research
School of Civil Engineering
National Technical University of Athens (NTUA)
Greece

COMPdyn 2025

Computational Methods in Structural Dynamics and Earthquake Engineering

M. Papadrakakis, M. Fragiadakis (Eds.)

First Edition, November 2025

© The authors

ISBN (set): **978-618-5827-06-9**

ISBN (vol II): **978-618-5827-05-2**

PRELIMINARY FINITE ELEMENT ANALYSIS OF A MODULAR AND STANDARDIZED CONNECTION BETWEEN EXISTING BUILDING AND EXOSKELETON

Michele Bianchessi¹, Simone Labò¹, Alessandra Marini¹, Andrea Belleri¹, and Chiara Passoni¹

¹ University of Bergamo
Department of Engineering and Applied Sciences
Dalmine (BG), Italy

{michele.bianchessi, simone.labo, alessandra.marini, andrea.belleri, chiara.passoni}@unibg.it

Abstract

Integrated, preferably holistic and externally implemented measures have proven to be effective in meeting the multiple needs of existing buildings, including structural, energy and architectural aspects. To achieve true economic, environmental and social sustainability throughout a building's life cycle, new performance objectives - such as durability, reparability and reusability - must be pursued alongside mandatory targets such as energy efficiency and structural safety. Recent studies have shown that enabling technologies are needed for achieving these new performance objectives. In this scenario, rethinking the role of connections, aiming at standardization and modularity, ease of implementation/replacement, activation/deactivation, proves to be a key strategy to improve the sustainability of both innovative and traditional retrofit measures. This study presents the preliminary results of the finite element analysis of a modular and standardized connection between an existing building and an exoskeleton. The finite element model validated the conceptual design and behavior of the connection.

Keywords: Enabling technologies, Integrated holistic interventions, Sustainability, Life Cycle Thinking, Finite Element Modeling, Renovation strategy.

1 INTRODUCTION

It is acknowledged that a significant renovation of the building stock is required to achieve the EU's ambitious targets for sustainability, safety, and resilience. Despite the urgency of the situation, the current renovation rate remains as low as 1%. To effectively achieve sustainability, this rate must be increased by identifying and addressing the key barriers to renovation. The Building Performance Institute Europe (BPIE) has identified several key obstacles to renovation, including the temporary relocation of tenants, the extended downtime required for construction work, the high costs of interventions, and the lack of suitable business models to support large-scale renovation efforts [1-2].

In order to overcome the main barriers to the renovation and pursue the effective sustainability of the building stock, innovative integrated interventions and retrofitting strategies such as an incremental rehabilitation plan designed according to the Life Cycle Thinking (LCT) principles have been studied and developed [3-4-6-8].

Integrated holistic interventions address structural, energy, and architectural aspects simultaneously, leading to a comprehensive enhancement of building performance and reducing the construction time [3,4]. Incremental rehabilitation strategies allow retrofitting measures to be phased over time, optimizing costs and construction time while ensuring progressive performance improvements [5-6].

Among possible enabling technologies that may foster LCT-oriented design, connections are acknowledged as key to facilitating and enabling the implementation of a sustainable, LCT-based retrofit system. Without re-engineering the connections, substantiating LCT performance objectives would be difficult, if not impossible. Structural connections, if designed according to Life Cycle Thinking (LCT) principles, not only need to ensure mechanical compatibility with the existing structure but also significantly influence the overall structural performance. In many cases, connections are key determinants of a building's global behavior, affecting aspects such as stiffness, energy dissipation, and load distribution [7,8,9,10]. Nevertheless, further investigation is required into the role of connections in enhancing the sustainability of retrofit solutions, given that only a limited number of authors have addressed the significance of connections regarding the environmental impact of buildings [11,12,13].

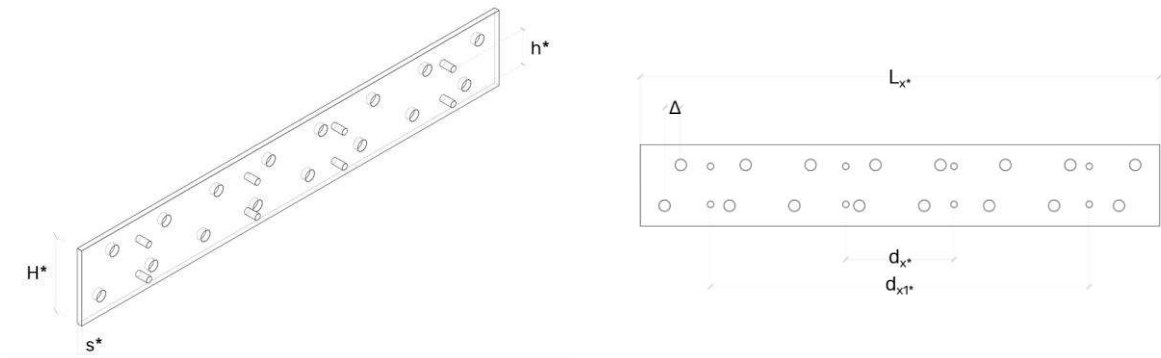
This paper presents the conceptual design and the preliminary finite element model (FEM) of a modular, plug and play, reversible, and standardized connection between an existing building and an exoskeleton. The connection is conceived to streamline easy assemblage, guarantee lumped damage and ease of reparability in the case of extreme events such as an earthquake, incremental implementation, deconstruction, and reusability of components at the end of life. The study aims to validate the conceptual design and assess its mechanical behavior.

2 CONCEPTUAL DESIGN OF THE CONNECTION

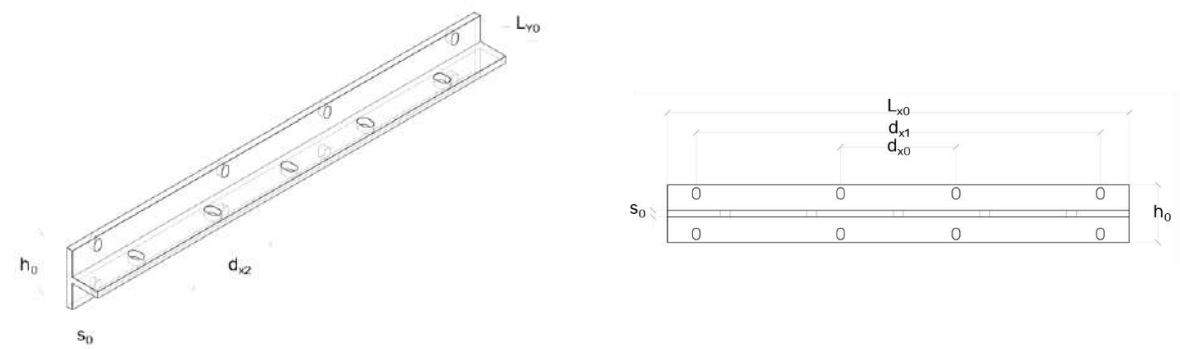
The present study focuses on the system that connects the horizontal floor of an existing building (floor slab band) to a steel exoskeleton. The proposed connection was developed based on the hypotheses outlined in [14]. The connection has been designed following Life Cycle Thinking (LCT) principles, incorporating modularity, prefabrication, standardization, and ease of assembly and disassembly [14]. These design choices enhance adaptability of the retrofit solution, enable incremental implementation, and potential for reuse of components at the end of the service life.

The connection components are shown in Figure 1 and are designed for easy assembly. Each component weighs less than 25 kg is standardized and modular. The system consists of four prefabricated elements, manufactured in a controlled environment to ensure precision and quality; namely:

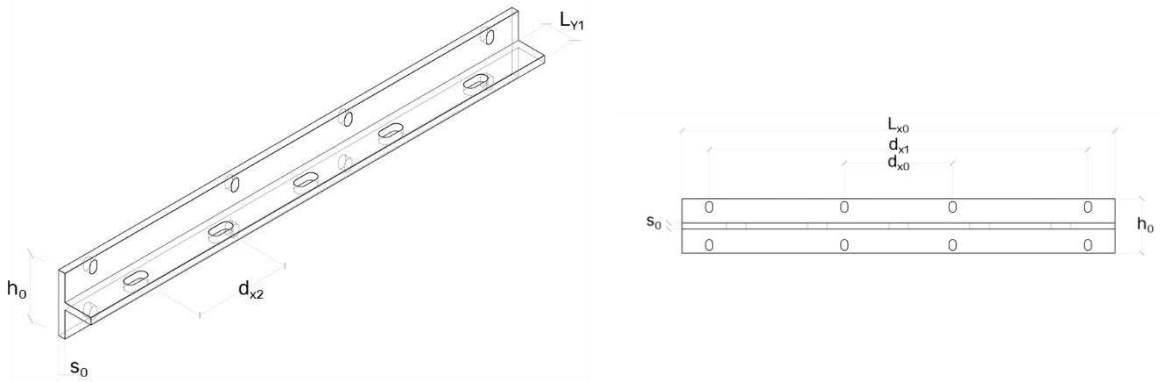
Element 0



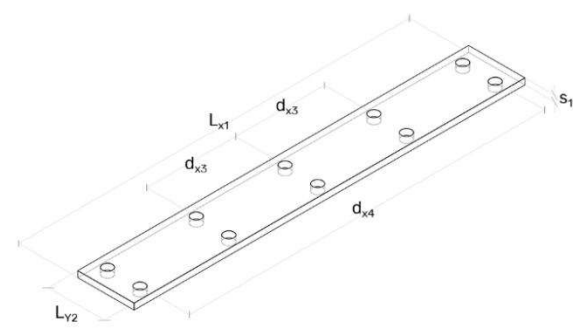
Element 1



Element 2



Element 3



Element 4

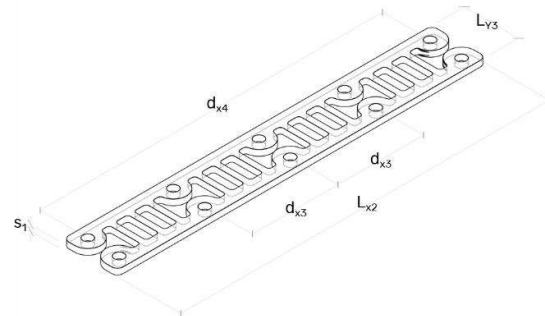


Figure 1 - Components of the connection system

Element 0: A pre-drilled steel plate, s^* thick and H^* high; the bottom and upper hole alignments are shifted by Δ to account for possible repositioning of the Element 0-to-RC side beam connectors (studs) in the case of interferences with RC corbel beam stirrups [14]. On the steel plate eight bolt shanks are welded. The central bolts are spaced 200 mm (d_{x^*}) and the outer bolts are spaced 700 mm (d_{x1^*}).

Element 1: A T-profile with sharp edges (100×100×11 mm) with a length (L_{X0}) of 800 mm, height (h_0) of 100 mm, width (L_{Y0}) of 50 mm, and thickness (s_0) of 11 mm. The vertical surfaces contain eight slotted holes ($\varnothing 13$ mm, 20 mm length) arranged with central holes spaced at 200 mm (d_{X0}) and outer holes at a 700 mm pitch (d_{X1}). The horizontal surface includes five slotted holes ($\varnothing 17$ mm, 26 mm length) with a spacing of 150 mm (d_{X2}). Hole-bolt clearances of ± 5 mm, streamline construction in the presence of construction tolerances.

Element 2: A T-profile with sharp edges (100x100x11 mm), with a length (L_{X0}) of 800 mm, height of 100 mm (h_0), width of 46 mm (L_{Y1}), and thickness of 11 mm (s_0). The vertical surfaces have eight slotted holes ($\varnothing 13$ mm, 20 mm length) in the same configuration as Element 1, while the horizontal surface contains five slotted holes ($\varnothing 17$ mm, 36 mm length) with a spacing of 150 mm (d_{X2}). Hole-bolt clearances of ± 10 mm, streamline construction in the presence of construction tolerances.

Element 3: A pre-holed plate with a thickness (s_1) of 10 mm, length (L_{X1}) of 660 mm, and width (L_{Y2}) of 95 mm. The holes have a diameter of $\varnothing 17$ mm and are spaced 150 mm apart (d_{X3}). The distance between the outermost holes (d_{X4}) is 600 mm.

Element 4: A laser-cut shaped plate with a thickness (s_1) of 10 mm, length (L_{X2}) of 646 mm, and width (L_{Y3}) of 95 mm. The holes have the same geometric characteristics as those in Element 3.

In the context of non-linear connection applications, Element 4 substitutes Element 3. Specifically, Element 4 functions as a custom-designed device conceived to dissipate energy through the controlled yielding of steel slats. The number of slats can be calibrated to attain target stiffness and resistance, thereby tailoring the connection's mechanical response to specific performance requirements.

3 STRUCTURAL CONCEPT

3.1 Elastic connection

The connection system has been engineered to effectively transfer inertial forces from the existing building to the exoskeleton, as depicted in Figure 2. Inertia forces are transferred from the RC chord to Element 1, through the steel studs and eight M12 class 10.9 bolts ($V_{Rd} = 42$ kN each). Shear actions are subsequently transmitted from Element 1 to the two steel plates (Element 3) by five M16 class 10.9 bolts ($V_{Rd} = 157$ kN each). Additionally, the rigid joint formed by two steel plates (Element 3) transfers the forces to Element 2 through another set five M16 class 10.9 bolts ($V_{Rd} = 157$ kN each). To ensure activation and enable the system to function through frictional resistance, the vertical connecting bolts require controlled tightening to target preloading. Each bolt is preloaded with $F_{PC} = 100$ kN, applied by imposing a torsional moment

of $M_r = 255$ kNm. At the end of the load path, the forces are transferred from Element 2 to the exoskeleton by eight M12 class 10.9 bolts ($V_{Rd} = 42$ kN each).

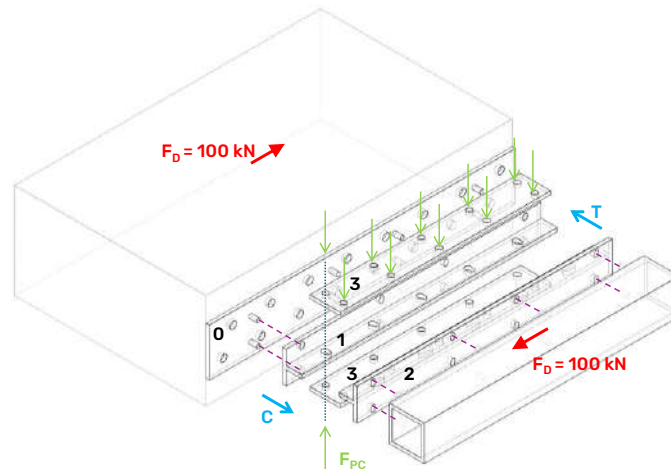


Figure 2 - Conceptual design of the connection system: elastic behavior

During the design phase, shear and bending actions were decoupled, and distinct functions were assigned to different structural elements. This was made to optimize the structural response of the components. Specifically, the connection was designed to transfer shear forces. Since the exoskeleton will not be installed in direct contact with the existing building, it is necessary to account for the eccentricity between the force acting on the beam and that acting on the exoskeleton. This condition gives rise to torsional effects in the exoskeleton, manifested as a combination of compression (C) and tension (T) forces, as depicted in Figure 2 and Figure 3. The latter forces are resisted by dedicated tie rods embedded within the RC chord and connected to the steel structure.

3.2 Non-linear connection

The connection is assembled as in the case of elastic system (section 3.1) as per Elements 0, 1 and 2 (Figure 1); whereas Elements 3 are substituted with Elements 4. Subsequently, the dissipative devices (Elements 4 in Figure 1) transfer the forces to Element 2 through five M16 class 10.9 bolts.

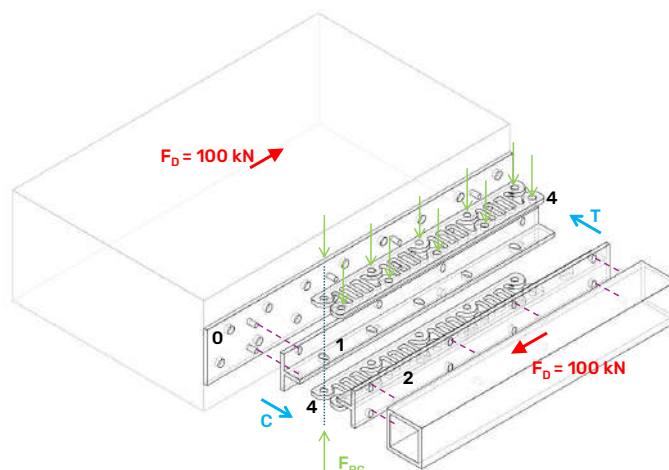


Figure 3 - Conceptual design of the connection system: non-linear behavior

The calibration of the dissipative device's strength and elastic stiffness is contingent upon the target design performance. These parameters can be adjusted through modification of the number and thickness of the thin steel slats.

4 FINITE ELEMENT MODEL

In order to investigate the behavior of the connection in both elastic and non-linear configurations, two finite element models were developed. The purpose of the present model was to validate the outcomes of the structural concept study of the connection between the existing building and the exoskeleton. The system was designed for a design force of $F_D = 100$ kN, as per the criteria outlined in [14]. The applied loads and the constraints of the mesh were defined to mimic the static and kinematic conditions of the connection in the real case application.

4.1 Elastic connection

The model was created by simulating a 960 mm-long structural element. The RC chord cross-section was defined with dimensions of 600×300 mm, while the exoskeleton element was modeled as a hollow steel profile measuring 110×110×10 mm. The connection was composed of Element 1, Element 2, and Element 3 described above.

The materials used in the model were concrete C25/30, with a characteristic compressive strength $f_{ck} = 25$ MPa, steel S275JR, with a design yield strength $f_{yd} = 275$ MPa, and 10.9 steel bolts, with a design yield strength $f_{yd} = 900$ MPa, as summarized in Table 1.

Table 1 - Materials of the connection systems

Description	Symbol	Value
Unconfined concrete strength	F_{ck}	25 MPa
Concrete Elastic Modulus	E_c	30000 MPa
S275 yielding stress	F_{yd}	275 MPa
S275 ultimate stress	F_u	430 MPa
S275 Elastic Modulus	E_s	200000 MPa
Bolt yielding stress	F_{yd}	900 MPa
Bolt ultimate stress	F_u	1050 MPa
Bolt ultimate strain	ε_u	1.5%
Bolt Elastic Modulus	E_s	200000 MPa

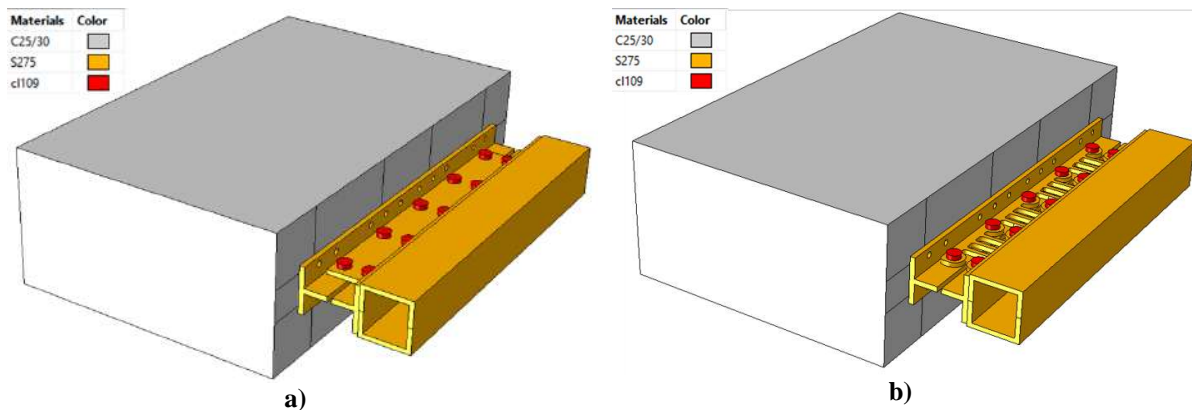


Figure 4 - Assignment of materials: a) Elastic connection b) non-linear connection

In this model, the RC chord is constrained with fixed supports at both ends. As for the exoskeleton, a sliding support condition has been applied at both ends, allowing movement along the longitudinal axis only. It is worth noting that alternative boundary conditions should be investigated in future studies.

Assumptions were made in the modelling of the contacts and connections between the system's components. The RC beam-to-Element 1 connection was modelled with rigid connectors, which represented a preliminary simplification to replace the explicit modelling of M12 bolts ($V_{Rd} = 42$ kN each). The rigid connection was assumed between Element 2 and the exoskeleton.

The bolted connections among Elements 1, 2, and 3 were explicitly modelled. The structural integrity of the assembly was ensured by applying a preload force $F_{PC} = 100$ kN to each bolt. The friction-based connection was modeled through a Coulomb friction model, with a friction coefficient (μ) of 0.4. This property was applied uniformly across all contact interfaces among Elements 1, 2, and 3. Additionally, tangential behavior was specified at the interface between the bolt head and Element 3 to accurately represent the load transfer mechanisms. Finally, a normal contact behavior with "hard contact" properties was modeled for all contact surfaces, ensuring a zero-penetration condition between the elements.

In order to evaluate the behavior of the connection beyond the design force ($F_D = 100$ kN), an overproportioning factor of 3 was chosen.

The RC chord cross-section was discretized using hexahedral elements (C3D8), while the steel profiles were modeled with tetrahedral elements (C3D10). This choice was made based on a sensitivity analysis. In the initial phase, a mesh refinement study was conducted. This involved varying the mesh size while maintaining the integration method of the individual elements. To optimize computational efficiency, the study was carried out using 3D tetrahedral elements with a linear integration method (C3D4). As shown in Figure 5, a comparison between models with mesh sizes (ms) of 5 mm and 2.5 mm revealed negligible variations in stiffness (k_{el}). Therefore, a mesh size of $ms = 5$ mm was adopted for subsequent simulation steps.

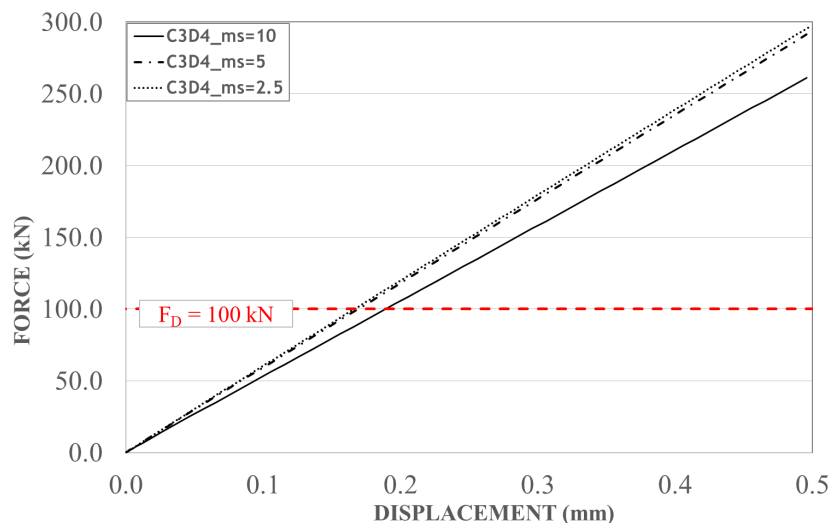


Figure 5 - Results of the analysis changing FE size

Additionally, the connection response was investigated by varying the integration method used in the finite element analysis. For tetrahedral elements, the behavior of the connection was evaluated by comparing models with first-order (linear integration) and second-order (quadratic integration) elements.

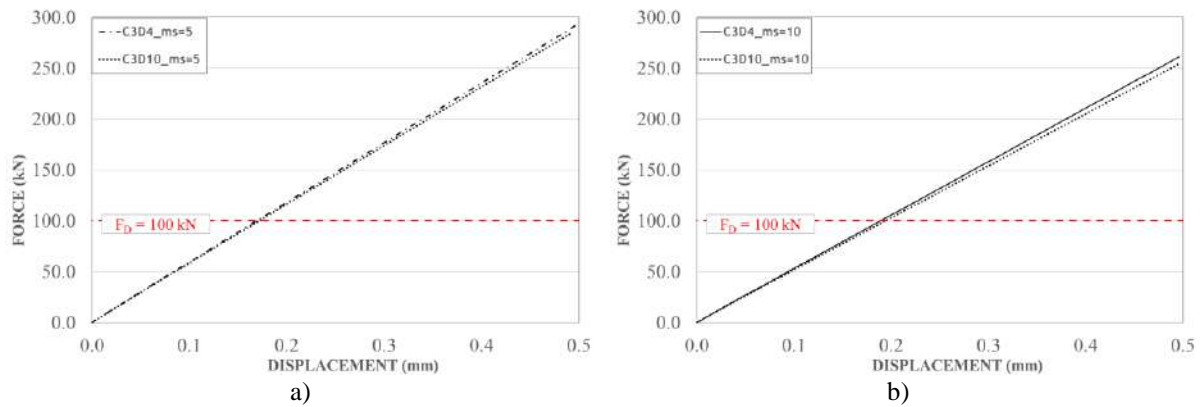


Figure 6 - Results of the analysis changing the integration methods

As demonstrated in Figure 6-a), the outcomes obtained from models with a mesh size of 10 mm are presented. Evaluating the stiffness (k_{el}), a 2.8% variation is observed depending on the integration method employed. The model developed with C3D10 elements exhibits lower stiffness. In Figure 6-b), the results from models with a mesh size of 5 mm are shown. In this case, the difference in stiffness between the two models is 0.8%, indicating an almost negligible influence of the integration method at a finer mesh resolution.

4.2 Non-linear connection

The development of the non-linear model was based on the elastic model described previously. The connection between these components is made using Elements 1, 2 and 4.

Similarly to the elastic connection described above, the connections between the RC chord and Element 1 and the exoskeleton and Element 2 are modelled using rigid connectors. The force transfer between the existing building and the exoskeleton is provided by the bolted connection of Elements 1, 2 and 4. As in the previous case, a steel-to-steel friction coefficient of $\mu_s = 0.4$ was considered. This property was assigned to all interfaces between Elements 1, 2 and 4 to accurately simulate the frictional interaction.

Based on the sensitivity analysis results obtained from the elastic model, the nonlinear connection behavior was studied by varying the mesh size. Figure 7-a) presents the results obtained from models with mesh sizes of $ms = 10$ mm and $ms = 5$ mm. In both cases, a second-order integration method was adopted using C3D10 elements. In accordance with the outcomes derived from the elastic model analysis, a mesh size of 5 mm was determined to be optimal. Additionally, the connection response was investigated by varying the integration method used in the finite element analysis. For tetrahedral elements, the behavior of the connection was evaluated by comparing models with C3D4 (linear integration) and C3D10 (quadratic integration) elements. The results obtained from models with different integration methods are depicted in Figure 7-b).

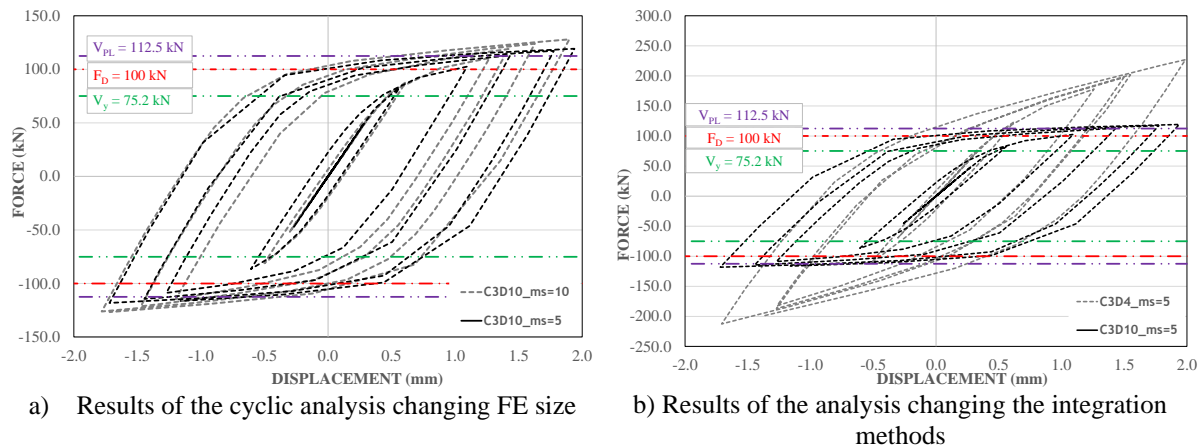


Figure 7 - Results of the cyclic analysis changing FE size

As shown in Figure 7-a), the results confirm that, as expected, finer mesh discretization results in greater accuracy for the same integration method. Specifically, the model with a mesh size of 5 mm produces outcomes that are in agreement with the expected results from the design phase.

However, a significant discrepancy becomes apparent when analyzing the results shown in Figure 7-b). A detailed examination of the curves in the nonlinear regime reveals that the model employing C3D4 finite elements (linear integration) demonstrates greater stiffness compared to the model using C3D10 finite elements (quadratic integration). This phenomenon can be attributed to the occurrence of volumetric locking, a well-documented issue in the literature when utilizing a tetrahedral mesh with linear integration methods. Conversely, the quadratic integration method yields results that are less prone to such effects [15].

4.3 Comparison of elastic connection and non-linear connection

Once the sensitivity analyses were completed, a comparison was made between the elastic and non-linear connections. The results validated the preliminary hand calculations, confirming that the elastic connection remains within its capacity even during an exceptional seismic event where the applied load is three times the design force. Regarding the non-linear connection, the analysis confirmed its ability to limit the transmission of forces above $F_D = 100$ kN, ensuring that damage is localized within the dissipative devices during an exceptional seismic event. Upon analysis of the stiffness of the elastic branch of the two connections, it was determined that the nonlinear connection exhibited a stiffness equal to 1/3 of the stiffness of the elastic connection. It is important to note that achieving identical stiffness in both configurations would have been feasible by reducing the plate thickness in the elastic configuration. This highlights the inherent design flexibility of the standardized connection system.

The ratio α between the elastic and post-yielding stiffness of the nonlinear connection is 1/35. The results are shown in Figure 8. It must be noted that this configuration is provided for illustrative purposes only, and elements 3 and 4 can be reconfigured as required to achieve specific performance objectives, provided that no other critical points emerge in the structure.

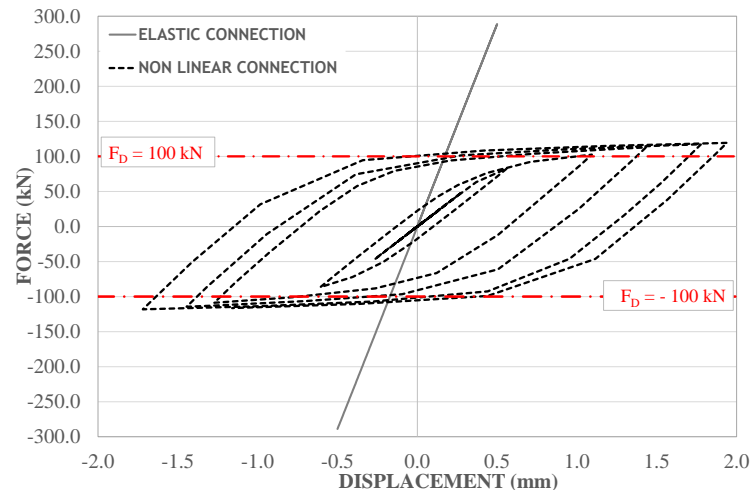


Figure 8 - Results of cyclic analysis comparing elastic connection with nonlinear connection

5 CONCLUSIONS

This study is part of ongoing research that aims to shift from a traditional to a life-cycle structural engineering approach, focusing on the conceptual design of a connection system between an existing building and an exoskeleton. In addition to mandatory requirements such as structural safety, the connection must also account for local construction tolerances, enable lumping the structural damage, ensure flexibility and incremental implementation, as well as deconstruction at the end of its service life.

In this work, both the structural concept and the behavior of the elastic and nonlinear connections were investigated through finite element models.

A sensitivity analysis was conducted by varying both the mesh size and the numerical integration method. The results from the elastic connection provided insights into the minimum required mesh element size, while the nonlinear analyses emphasized the necessity of modeling finite elements using a second-order integration method. Neglecting this aspect can lead to inaccuracies in determining the stiffness of the nonlinear connection.

The results confirmed that the elastic connection maintains an elastic response even under forces much greater than the design load, as long as the collapse mechanism governed by the capacity design relies on the yielding of different structural elements. For the nonlinear connection, the study showed that the maximum force transferred from the existing building to the exoskeleton remains equal to the design force, ensuring the intended damage localization in the dissipative devices.

Future developments will require an in-depth investigation of the global behavior of the connection. A further key aspect for future research involves further analysis of the connection's response under different boundary conditions. In addition, future research activities will focus on the design and testing of a physical prototype.

REFERENCES

- [1] BPIE 2011, Europe's buildings under the microscope: A country-by-country review of the energy performance of the buildings (Brussel), 2011.
- [2] P. La Greca, G. Margani, Seismic and Energy Renovation Measures for Sustainable Cities: A Critical Analysis of the Italian Scenario. *Sustainability*, **10(1)**, 254, 2018.

- [3] A. Marini, Coupling energy refurbishment with structural strengthening in retrofit interventions, *SAFESUST Workshop 2015 - A roadmap for the improvement of earthquake resistance and eco-efficiency of existing buildings and cities*, Ispra, 2015.
- [4] A. Marini, C. Passoni, A. Belleri, F. Feroldi, M. Preti, G. Metelli, E. Giuriani, G. Plizzari, Combining seismic retrofit with energy refurbishment for the sustainable renovation of RC buildings: a proof of concept. *European Journal of Environmental and Civil Engineering*, 2017.
- [5] FEMA P-420, Engineering Guideline for Incremental Seismic Rehabilitation. *United States. Federal Emergency Management Agency*. FEMA disaster program information. Washington, DC:FEMA, 2009.
- [6] J. Zanni, S. Cademartori, A. Marini, A. Belleri, C. Passoni, E. Giuriani, P. Riva, B. Angi, G. Brumana, A.L. Marchetti, Integrated Deep Renovation of Existing Buildings with Prefabricated Shell Exoskeleton. *Sustainability*, **13(20)**, **11287**, 2021.
- [7] J. Kelly, R. Skinner, A. Heine A, Mechanisms of energy absorption in special devices for use in earthquake resistant structures. *Bulletin of New Zealand Society for Earthquake Engineering*, **5(3)**, 1972.
- [8] G. Rodgers, J. Chase, J. Mander, N. Leach, C. Denmead, Experimental development, tradeoff analysis and design implementation of high force-to-volume damping technology. *Bulletin of the New Zealand Society for Earthquake Engineering*, 2006.
- [9] K. C. Tsai, C. P. Hong, Steel triangular plate energy absorber for earthquake-resistant buildings. *Constructional Steel Design: World Developments, Elsevier Applied Science*, **529-540**, 1992.
- [10] A. Whittaker, V. Bertero, C. Thompson, L. Alonso L., Seismic testing of steel-plate energy dissipating devices. *Earthquake Spectra*, **7(4)**, **563–604**, 1991.
- [11] B.A. Burgan, M. R. Sansom, Sustainable steel construction. *Journal of Constructional Steel Research*, **62 (11)**, **1178-1183**, 2006. <https://doi.org/10.1016/j.jcsr.2006.06.029>
- [12] S.S. Shilavantar, S. Suthar, B. Chaitanya, A. Chiranth, R. Ravindra, Sustainability by Reverse Joints in Steel Structures (Demountable Modular Shear Connection). In: M. Madhavan, J.S. Davidson, N.E. Shanmugam, (eds), Proceedings of the Indian Structural Steel Conference 2020 (Vol. 2). ISSC 2020. Lecture Notes in Civil Engineering, **vol 319**. Springer, Singapore, 2023.
- [13] C. Passoni, A. Marini, A. Belleri, C. Menna, Redefining the concept of sustainable renovation of buildings: State of the art and an LCT-based design framework, *Sustainable Cities and Society*, **Volume 64**, 2021.
- [14] S. Labò, J. Zanni, A. Marini, Rethinking the role of the connections to improve the sustainability of the retrofit actions. *Proceedings of World Conference on Earthquake Engineering (18WCEE)*, Milan, Italy, 2024.
- [15] ABAQUS analysis user's manual (Academic version 2022). Dassault Systèmes, 2022.